

Matching of Radiation with Array of Planar Antennas with SINIS Bolometers in an Integrating Cavity¹

M. A. Tarasov^a, A. M. Chekushkin^{a, *}, R. A. Yusupov^a, A. A. Gunbina^{b, c}, and V. S. Edelman^d

^a*Institute of Radioengineering and Electronics, Russian Academy of Sciences, Moscow, 125009 Russia*

^b*Nizhny Novgorod State Technical University, Nizhny Novgorod, 603950 Russia*

^c*Institute of Applied Physics, Russian Academy of Sciences, Nizhny Novgorod, 603950 Russia*

^d*Kapitsa Institute for Physical Problems, Russian Academy of Sciences, Moscow, 119334 Russia*

*e-mail: chekushkin@hitech.cplire.ru

Received July 11, 2019; revised July 11, 2019; accepted July 19, 2019

Abstract—Arrays of planar annular antennas in the 345 GHz range with integrated superconductor–insulator–normal metal–insulator–superconductor (SINIS) bolometers have been developed, fabricated, and experimentally investigated. To increase the absorption efficiency, the source signal was matched with the array using a back-to-back horn and a counterreflector. The efficiency of the receiving structure was studied depending on the direction of irradiation—through the substrate and from the antenna—as well as on the thickness of the substrate. The methods for normalizing a received signal using a reference channel outside and inside a cryostat is described. The best results were obtained by irradiating the array from the antenna with a substrate thickness equivalent to a quarter wavelength in the dielectric and sputtering of the rear side with a gold film (counterreflector). The effective matching band in the main range was more than 50 GHz; the volt–watt sensitivity reaches 10^9 V/W.

DOI: 10.1134/S1064226920010064

INTRODUCTION

Currently, astronomy is actively developing in the millimeter and submillimeter wavelengths ranges. Research in this area is aimed at studying relict radiation, the “cold” Universe, star formation processes, and much more. For such problems, high-altitude ground-based, balloon, and space observatories have been created, e.g., ALMA, OLIMPO, Millimetron, etc. A signal collected by the telescope mirror is detected by highly sensitive detectors. When developing detectors for various observatories, one of the key tasks is matching the signal coming from the mirror to the detector. Various mirror, horn, and lens system designs can act as matching devices. This article presents an experimental study on matching the array of planar antennas with superconductor–insulator–normal metal–insulator–superconductor (SINIS) bolometers with external radiation using a back-to-back horn with a counter-reflector.

1. BACK-TO-BACK HORN WITH A COUNTER-REFLECTOR AS AN INTEGRATING CAVITY

A design involving back-to-back horn is used to match the detector with the telescope in a number of

radio astronomy instruments, e.g., the European Space Observatory Planck (ESA Planck project), the Italian balloon telescope OLIMPO, etc. As noted in the classical review [1], the absorption capacity of most bolometers is less than unity compared to a blackbody, and an integrating cavity must be used to increase the absorption efficiency of the incoming radiation. In such a cavity, there are many standing waves, which makes it very difficult to numerically analyze such a structure accurately, and therefore, experimental studies play a large role, the results of which are presented in this work. One approach, which uses the random photon model, was proposed in [2] for cavities of arbitrary shape with dimensions much larger than the wavelength. It is believed that a photon can be absorbed in several ways. With an arbitrary photon distribution, the absorption is proportional to the effective area of the blackbody, equal to the real area multiplied by the absorption capacity (degree of blackness). It is assumed that the effective area of the blackbody absorber is larger than the area of all openings and the effective blackness of the walls. From this aspect, the use of a light concentrator entails a decrease in the relative area of the matching hole. According to [3], the solid angle at which the bolometer sees its reflection on the walls of the cavity should be less than the solid angle at which it sees the source. If the cavity is illuminated by a partially collimated beam, the detector should be tilted so that the

¹ The work was awarded the prize at the 15th Ivan Anisimkin Competition for Young Scientists.

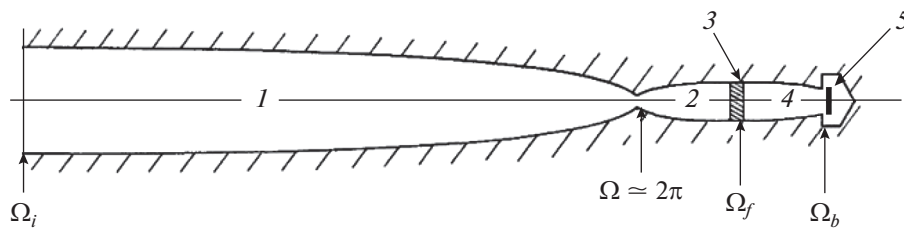


Fig. 1. Optical system design: (1) the Winston concentrator determining throughput $A\Omega$; (2) second concentrator; (3) irradiating filter; (4) third cone; (5) directly irradiating bolometer in third cavity.

reflected beam does not return to the outside, instead remaining in the cavity and being absorbed after multiple reflections. The classical design of such a system was developed in [4] (Fig. 1).

Another design with horns with an integrating cavity (Fig. 2) was implemented for the JCMT telescope and SCUBA bolometer [5]; it uses a direct horn and an array of 91 bolometers for ranges of 438 and 855 μm . Here, the need for long wires increases the area behind the bolometer to more than what is desirable for high optical efficiency.

One of the simplest integrating cavity designs is cylindrical (Fig. 3) [6], developed and manufactured at the Jet Propulsion Laboratory: Microdevices Laboratory of the California Institute of Technology. The absorption coefficient in such a chamber reaches 95% with crosstalk between pixels of less than 1% and a passband of $\Delta f/f = 0.33$. The resistance per square in the absorber can vary from 150 to 700 Ω .

Also noteworthy is the implementation of back-to-back corrugated horns for a center frequency of 90 GHz for the high-frequency instrument (HFI) COBRAS/SAMBA (later Planck) [7], where the passband was 25%, the length of the cylindrical part of the narrow single-mode circular waveguide was 2λ , and the radius was 0.6λ .

A detailed theoretical analysis of the operation of back-to-back horn was carried out in [8], where it was noted that a sharp jump in impedance at the edge of the waveguide and the integrating cavity leads to reflections and reduces the efficiency of matching with a broadband source. The use of a second smooth horn significantly improves the uniformity of the spectral characteristics. Such horns are used in the 550

and 850 GHz channels of the HFI PLANCK Surveyor Satellite space telescope. Figure 4a shows a sketch of this design; Fig. 4b, our design with back-to-back horn and a counter-reflector. Calculation of radiation pattern in the far zone is reduced to summation in quadratures, i.e., addition of the powers of all undamped modes. Numerical calculation shows that the expanding horns in the shape of a square of the sine yields the narrowest radiation pattern of such a single-mode horn, $\pm 5^\circ$. A comparable result can be obtained for a significantly longer right conical horn.

Thus, the integrating sphere or cavity is a simple solution to the problem of efficient matching in the case of focusing of the source signal on the detector. The main reasons for using the integrating cavity are as follows:

- the need to create a uniform radiation pattern (RP) for a detector with a heterogeneous RP;
- the need to ensure isotropic reception even by detectors with selective absorption directions;
- reduction of polarization effects due to the size/shape of the detector;
- the possibility of using the entire RP of the detector in the proposed structure, including the side and rear lobes.

The integrating sphere is a reflecting surface, and the detector is placed inside it, so that the signal entering the cavity is multiply reflected from the walls and, as a result, most of the incoming signal is absorbed by the detector. Thus, the integrating cavity increases the

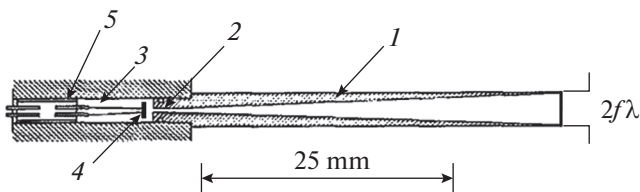


Fig. 2. Horn design with integrating cavity: (1) horn in form of right cone; (2) circular waveguide; (3) integrating cavity for NTD-Ge bolometer; (4) bolometer; (5) electrical feedthroughs.

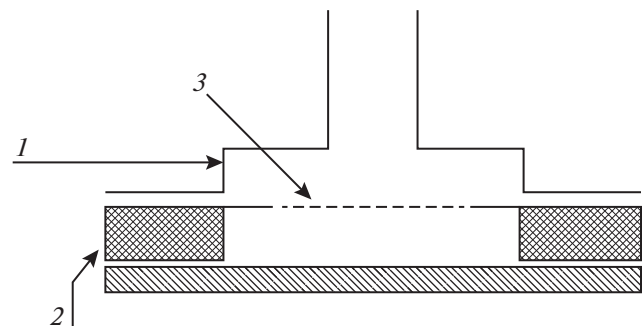


Fig. 3. Diagram of bolometric chamber 1 of 214 GHz band including silicon substrate 2 with thickness of $400 \mu\text{m}$ etched prior to metallization (absorber 3)

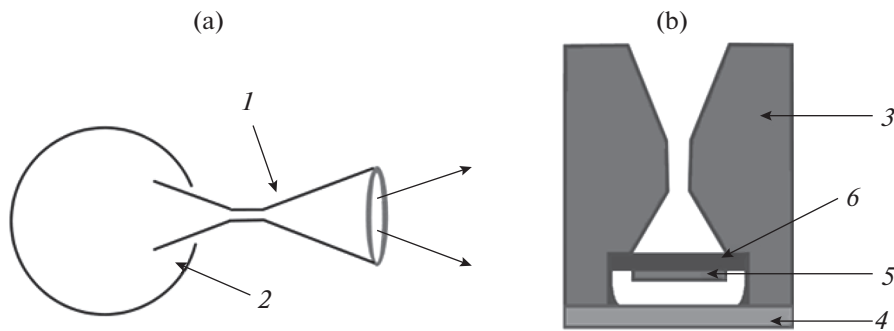


Fig. 4. Sketches: (a) horn matching device 1 of HFI with integrating cavity 2 of PLANCK Surveyor Satellite Space Telescope; (b) our design of back-to-back horns 3 and flat counter-reflector 4 array of planar antennas 5 with integrated SINIS bolometers on silicon substrate 6.

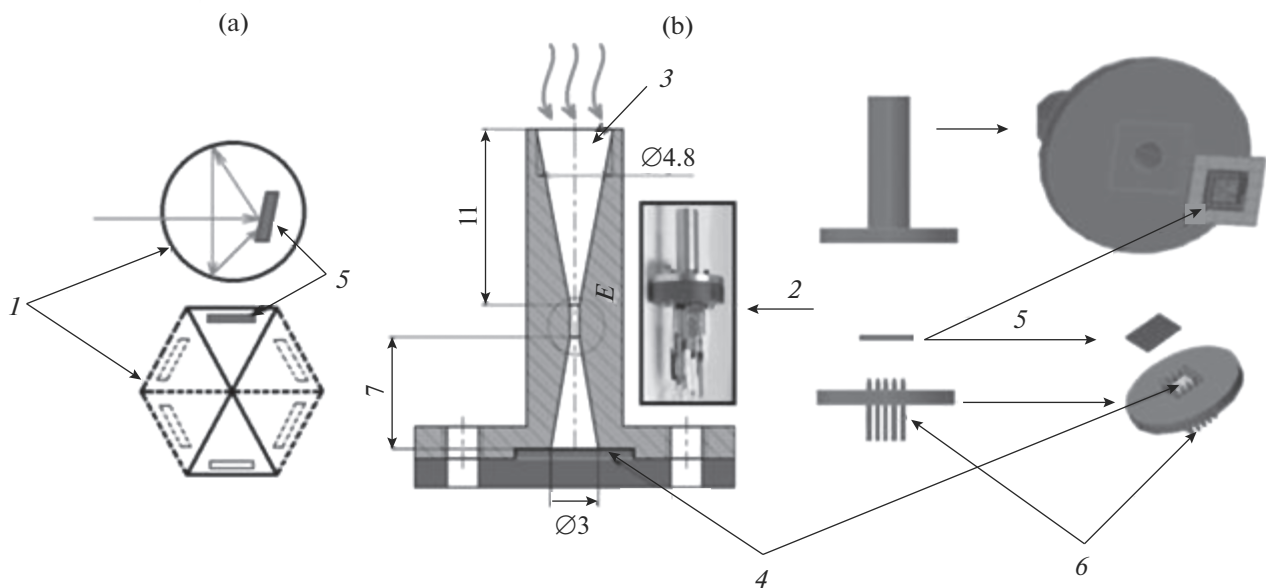


Fig. 5. Integrating cavity circuit 1 (a) and profile of 3D model of sample holder 2 (b) in form of back-to-back horns 3 with counter-reflector 4. Test sample 5 fixed in holder by means of pressure contacts 6.

detection efficiency of the signal due to multiplication of radiation entering the cavity. This improves matching of the incoming radiation with the detector. One of the characteristics of the integrating cavity is the coefficient of the sphere multiplier (M), which is associated with the coefficient of reflection from the walls (ρ_ω) and the ratio of the input window of the sphere to its total area by the following relations:

$$M = \rho_\omega / [1 - \rho_\omega(1 - f)],$$

for or $f = (A_w/A_s)$, $\rho_\omega = 1$, $M = A_s/A_w$. In practice, the input window area is about 5% of the total area of the sphere, the reflection from the walls is 95–99%, and the resulting coefficient of the sphere can be from 10 to 50. The flux density inside the integrating cavity is M times more than direct radiation.

In our case, the detector or annular antenna array with SINIS-bolometers is matched with the external

signal using the design with back-to-back horns connected by a circular waveguide with a diameter of 0.9 mm and length of 2 mm and a counter-reflector (Fig. 5), which is a certain equivalent of the integrating cavity. The signal from the source enters the horn, is multiply reflected from its walls and the counter-reflector, and is absorbed by the collecting array based on SINIS bolometers. The presence of metal walls can be considered as mirrors in which the image of our bolometer array is reflected (for a schematic image, see Fig. 5a).

2. ARRAYS OF PLANAR ANTENNAS WITH INTEGRATED SINIS BOLOMETERS

The SINIS bolometer is a thin absorber film made of a normal metal and two superconductor–insulator–normal metal (SIN) junctions (Fig. 6). The incoming radiation is absorbed by the absorber, as a

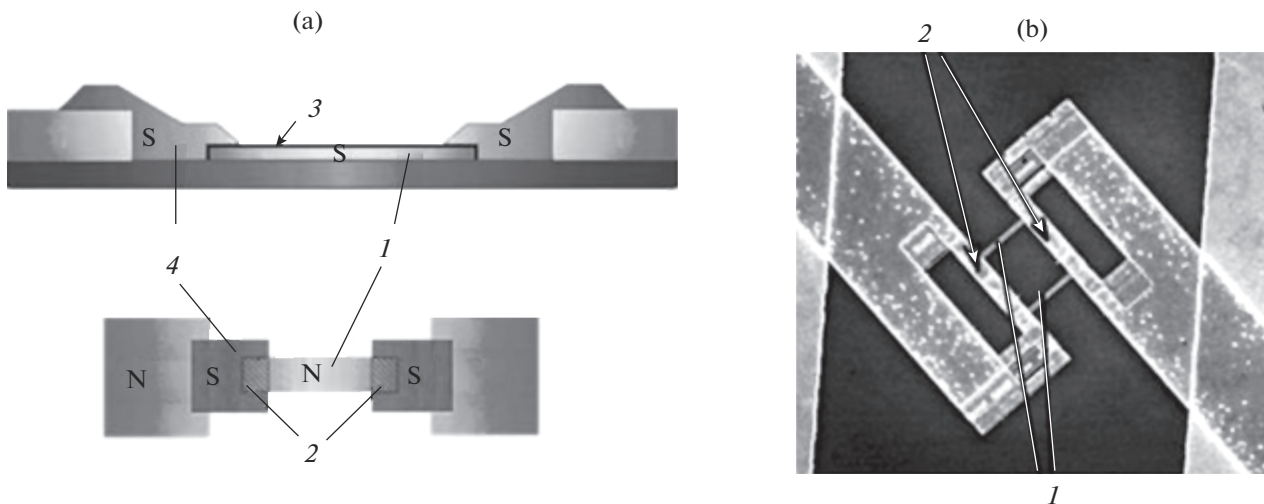


Fig. 6. Scheme (a) and photograph (b) of SINIS bolometer: (1) thin absorber film of normal metal (aluminum with iron sublayer); (2) two SIN transitions. Insulator layer (3) formed by oxidizing aluminum in chamber, followed by superconducting aluminum (4).

result of which its electronic temperature, measured by the SIN junction, increases.

Under operating conditions at real observatories, the background power reaches tens of picowatts. A single SINIS bolometer is saturated with absorbed power of less than 1 pW, but by combining dozens of such bolometers into an array, the saturation power can be significantly increased, since the incoming power will be distributed between the bolometers.

The developed structures were modeled in CST STUDIO SUITE. We were unable to simulate a real detector and compile a complete electrodynamic pattern due to the very large number of spatial modes. In the horn-counter-reflector system, there are a large number of reflections and interaction occurs between the 50 antennas of the array and the signal modes. We can perform approximate qualitative modeling for a preliminary assessment of the developed structures in order to determine some of the array parameters. All other corrections are introduced after experimental studies.

For the problems under consideration, a single array element must meet the following requirements: the absence of polarization selectivity, the ability to integrate SINIS bolometers, and the presence of an radiation pattern (RP) that does not form so-called substrate modes. As a single element, various antennas were considered: a circular, square, and *L*-antenna. The simulated RPs are shown in Fig. 7. Based on the results, we can conclude that the planar annular antenna (see Fig. 7a) satisfies the listed requirements better than others. In the case of *L*-antennas (see Fig. 7c), part of the pattern is oriented in the plane of the substrate, which will create substrate modes.

Having chosen a single element, we can combine such antennas into an array, a so-called frequency-selective surface [9].

The absorption efficiency of the incoming signal in the structures under development depends on the thickness of the substrate on which the antenna array has been manufactured, as well as on the distance to the counter-reflector. We have modeled (Fig. 8) the RP of an annular antenna on silicon substrates of various thicknesses Z_{sub} : $64.5 \mu\text{m} (\lambda^*/4)^2$, $129 \mu\text{m} (\lambda^*/2)$, 280 and $380 \mu\text{m}$ (standard substrate thicknesses). The half-wavelength substrate (see Fig. 8c) promotes the formation of substrate modes, which reduces the absorption efficiency of the incoming signal. The most optimal variant is a quarter-wavelength-thick substrate (see Fig. 8b). In practice, the silicon etching process in SF_6 gas is used to obtain the required thickness (see photo of substrate with etched membranes, Fig. 8f). Such a process is not always available, it is difficult to control, and, in addition, the substrate becomes brittle. If it is not possible to make an etched substrate, then it can be replaced with a standard one with a thickness of $380 \mu\text{m}$ (see Fig. 8e).

Such bolometric arrays are manufactured in three technological cycles: silicon etching; formation of the first layer, consisting of planar antennas, connecting wires, and pads; formation of the second layer, consisting of a bolometer array. The first layer can be made by electron (or laser) lithography, and then three layers are deposited by electron beam evaporation: $10 \text{ nm Ti}/100 \text{ nm Au}/20 \text{ nm Pd}$. The layer in which the SINIS bolometers are located is made using the shadow evaporation technique. The formation of a resistive mask for a layer with bolometers is carried out only by electronic lithography due to the small size of the absorber (the minimum size of bolometric structures is the width of the absorber, which is 100 nm). First, a thin film of a normal metal absorber (15 nm Fe/Al) is deposited at a right angle, then an insulator layer is formed by injecting oxygen into the

² λ^* is the wavelength in the dielectric.

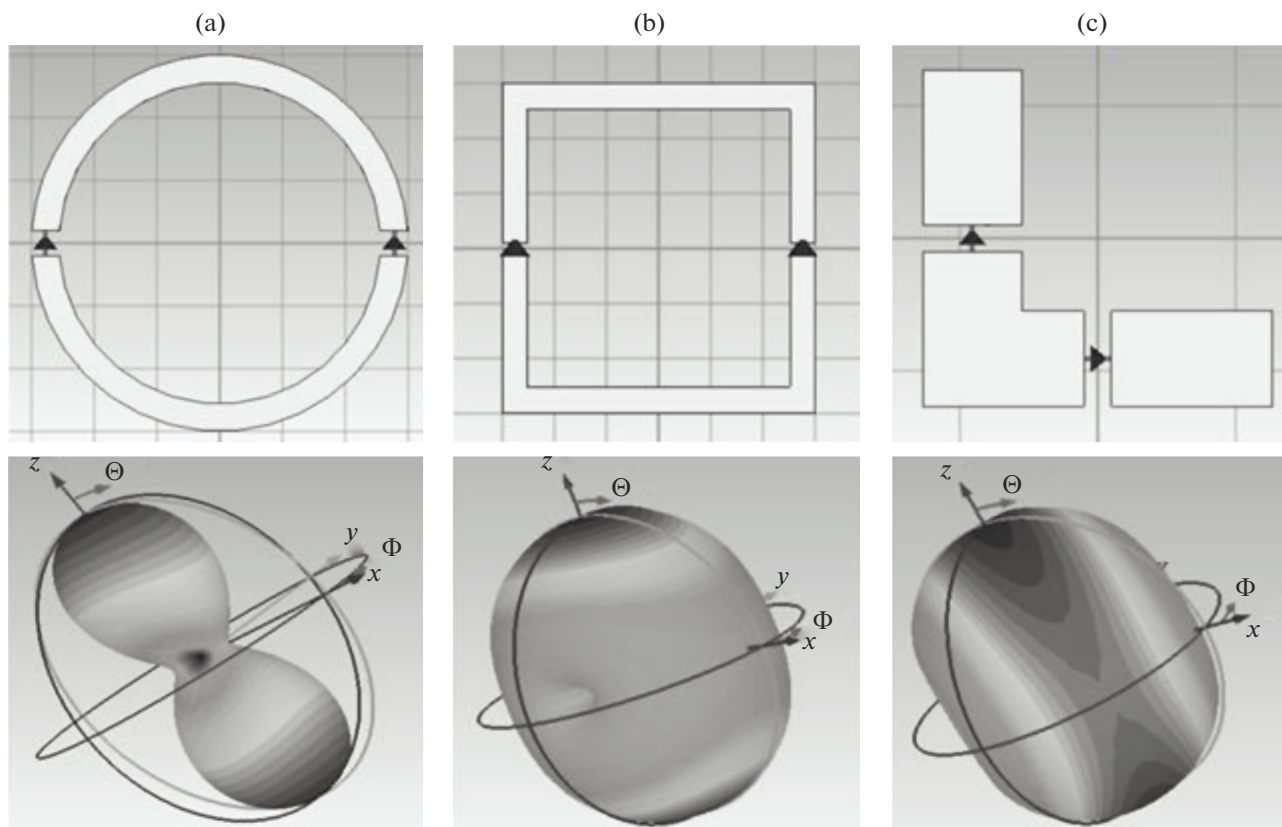


Fig. 7. Simulated structures (upper row) and resulting radiation patterns (lower row): (a) annular antenna; (b) square antenna; (c) L-antenna.

chamber, and then superconducting aluminum electrodes are deposited at angles of $\pm 45^\circ$.

Arrays of annular antennas were made, consisting of 25 annular planar antennas with two or four integrated SINIS bolometers. A 5×5 array of an annular antennas with a center frequency of 345 GHz fit geometrically into the opening of a horn with a diameter of 3 mm. Elements in the array can be connected both in series and in parallel, depending on which readout system is intended. Serial connection of elements ensures a high output asymptotic resistance (15 k Ω); in this case, at the operating point, the resistance of the array is about 500 k Ω and the readout system based on field-effect transistors with a semiconductor gate will be optimal. When the elements are connected in parallel, the normal array resistance will be about 15 Ω , which allows use of a superconducting quantum interferometer (SQUID) or bipolar transistor with a cryogenic matching transformer for measuring the signal. Photos of the manufactured samples are presented in Fig. 9.

3. METHODS FOR IRRADIATING A RECEIVING ANTENNA

Two types of irradiation of the annular antenna array were considered: through the dielectric substrate (Fig. 10a) [10] and from the antennas (Fig. 10b). In the

first case, during modeling, the counter-reflector was installed at a distance of $\lambda/4$. In practice, such a counter-reflector is a piece of aluminum tape glued to the sample holder (shown schematically in Fig. 5). In the second case, when the array is irradiated from the antennas, a counter-reflector was applied directly to the substrate from the rear side by sputtering a thick layer (100 nm) of gold. Computer simulation (Fig. 11) showed that the variant with irradiation from the antennas yields better results: a more uniform response and better matching. Comparison with experimental data is presented in the next section. To improve the uniformity of the spectral response in the case of irradiation from the dielectric substrate, an antireflection coating was used; in practice, two layers of Kapton adhesive tape were used as such a coating.

4. EXPERIMENTAL SETUP AND MEASUREMENT RESULTS

Schematic images of the experimental setups are presented in Fig. 12. The samples were measured at an operating temperature of 100 mK in an immersion dilution cryostat [11] and at 300 mK in a cryostat from Oxford Instruments—He3 Refrigerator—Heliox AC—V. A holder with a horn and a sample was mounted on the cold plate of the cryostat. Two types of measurements were carried out: the spectral response measurement, when a backward-wave oscillator (BWO) in the 230–

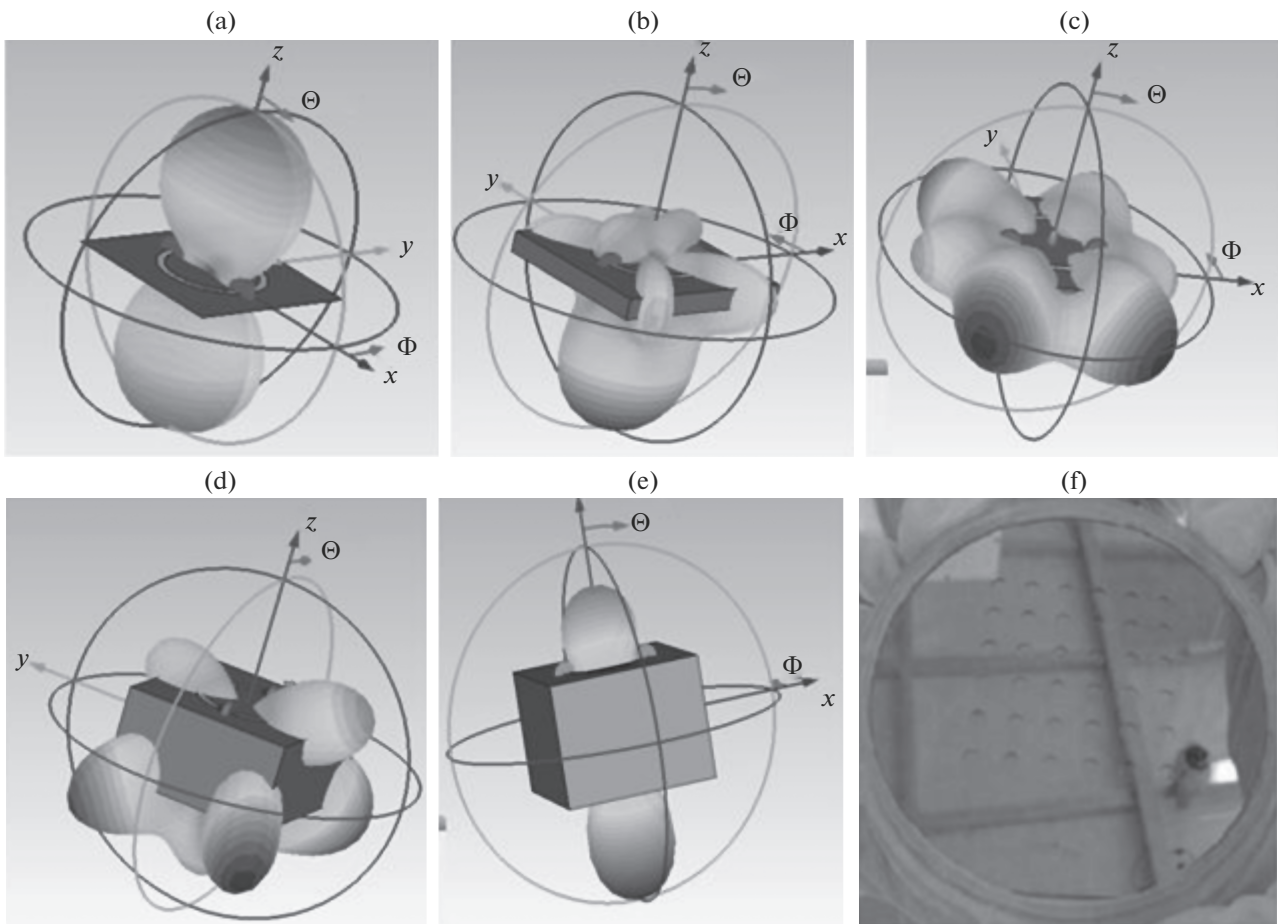


Fig. 8. Radiation patterns of annular antenna on silicon substrate of various thicknesses: $Z_{\text{sub}} = 0$ (a), 64.5 (b), 140 (c), 280 (d), 380 μm (e); and photograph of etched membranes (f).

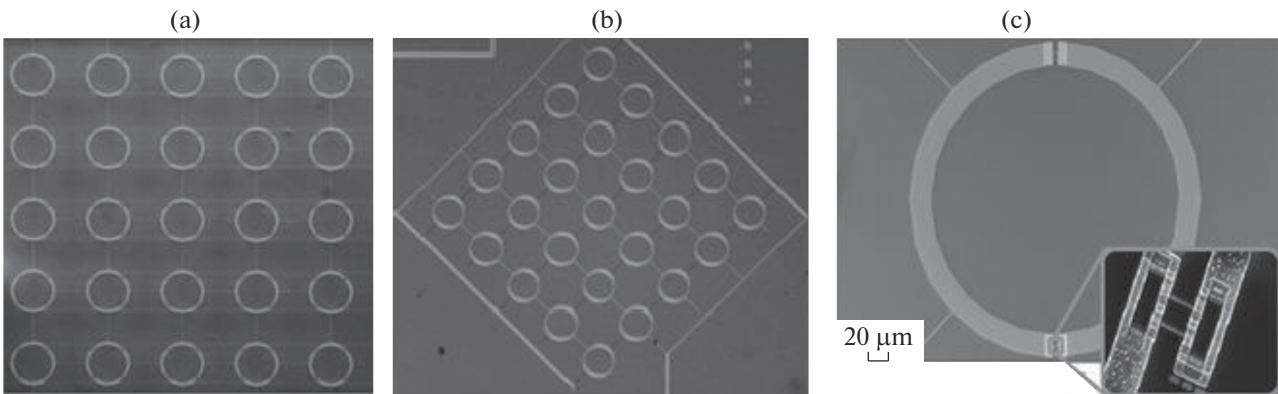


Fig. 9. Photos of manufactured bolometric arrays: (a) array with serial connection of elements, (b) array with parallel connection of elements, (c) single array element; inset, SINIS bolometer.

380 GHz range was used as the radiation source, and the optical response to blackbody (BB) radiation was measured.

4.1. Measurement of the Spectral Response

The signal from the radiation source in the room entered the sample through the three optical windows

in the cryostat (see Fig. 12a). At the same time, the signal from the bolometer and the reference signal from the BWO were detected with a pyroelectric detector, after which the signal from the bolometer was normalized to the reference signal. When studying the spectral response of arrays with different types of irradiation, to compare the level of the received signal, the samples were measured in a single experimental cycle (Fig. 13).

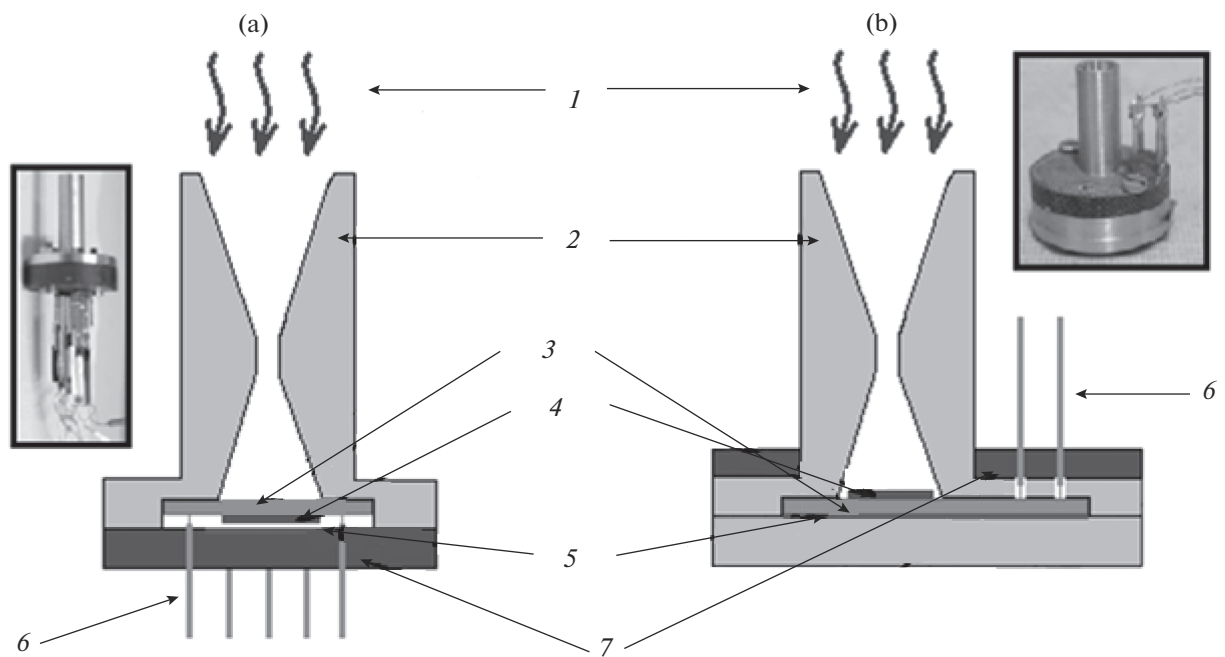


Fig. 10. Schematic representation and photographs of real samples for various methods of irradiating collecting array: (a) from silicon; (b) from antennas. (1) incoming radiation; (2) back-to-back horn; (3) silicon substrate; (4) collecting array; (5) counter-reflector; (6) clamping contacts; (7) fiberglass insert for gluing pressure contacts.

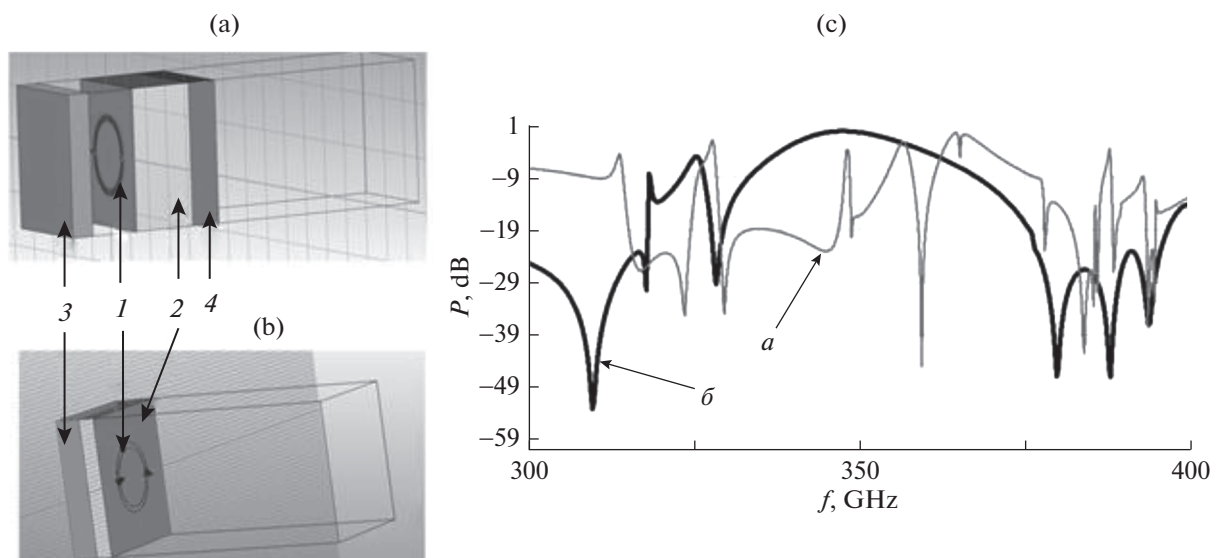


Fig. 11. External view of modeled structures through dielectric substrate (a) and from side of antennas (b): (1) annular antenna; (2) silicon substrate; (3) counter-reflector; (4) antireflection coating; and also simulation results (c) obtained, respectively, upon irradiation from side of antennas (b) and through dielectric substrate (a).

4.2. Optical Response Measurement

When measuring the optical response, a BB was used as a signal source—a thin nichrome film deposited on sapphire or silicon. The BB was mounted on the plate of the cryostat with a temperature of 0.5 K; it could be heated to 7 K. In order to “cut out” the necessary band from the BB radiation spectrum and eliminate the spurious IR illumination that overheats bolometers, bandpass filters were placed between the

signal source and the collecting array [12]. The measurement results are shown in Figs. 13b and 13c.

5. DISCUSSION

When measuring the spectral response, the signal from the radiation source (BWO) undergoes multiple reflections en route to the detector. In our early works, the signal measured from the bolometric array was normalized to the reference signal measured by a pyro-

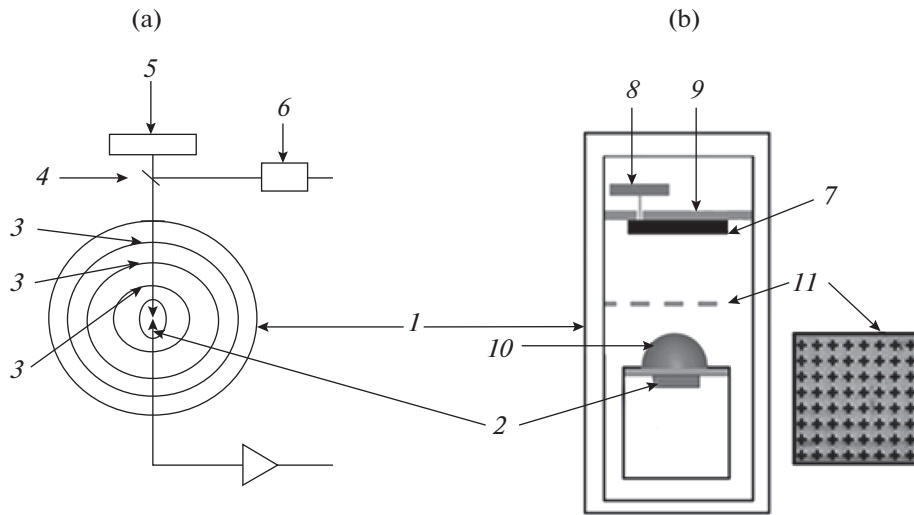


Fig. 12. Schematic representation of experimental setups: (1) cryostat (300 mK (a) and 100 mK (b)); (2) test sample; (3) optical filters in cryostat windows; (4) obturator-type modulator; (5) radiation source (BWO); (6) pyroelectric; (7) radiation source (BB); (8) heater; (9) plate of cryostat with temperature of 0.5 K; (10) lens; (11) bandpass filter.

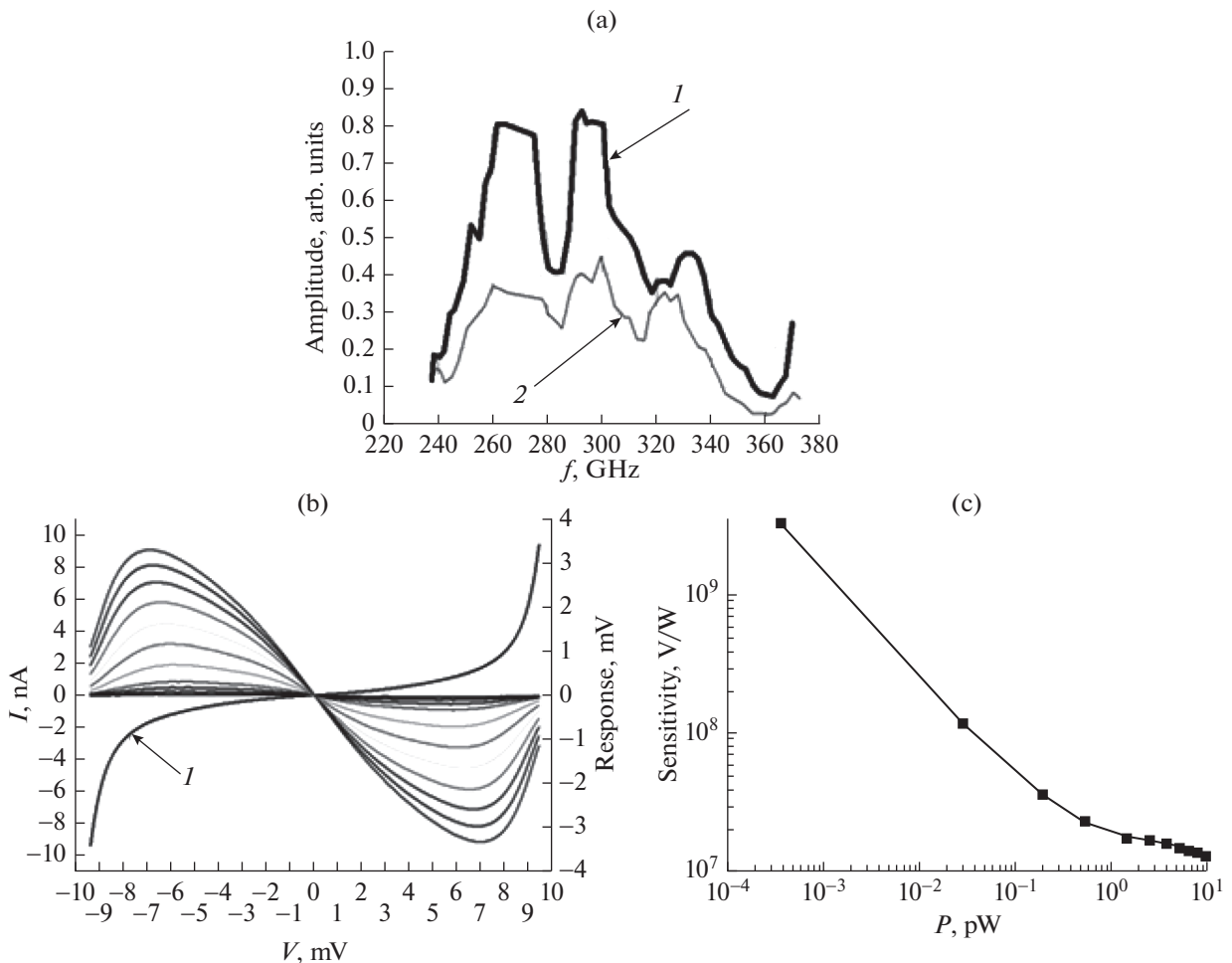


Fig. 13. Results of experimental measurements: (a) spectral response of samples to incoming signal from BWT in case of irradiation from antennas and through dielectric substrate; (b) response of array of serially connected elements to BB radiation of various temperatures, curves from lower to higher $-T_{bb}$ (in K): 0.7, 2, 3, 4, 6, 7.5, 9, 10.7, 12.4, 14, 15.5; in volt-watt sensitivity.

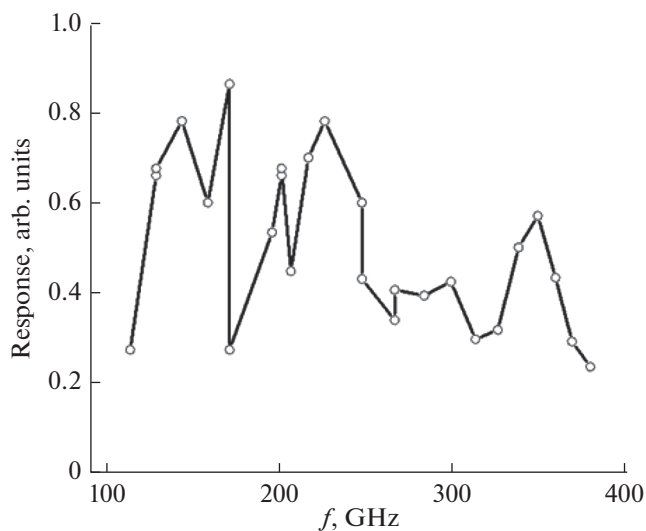


Fig. 14. Spectral response of 350 GHz array on sapphire lens in 100–400 GHz frequency range.

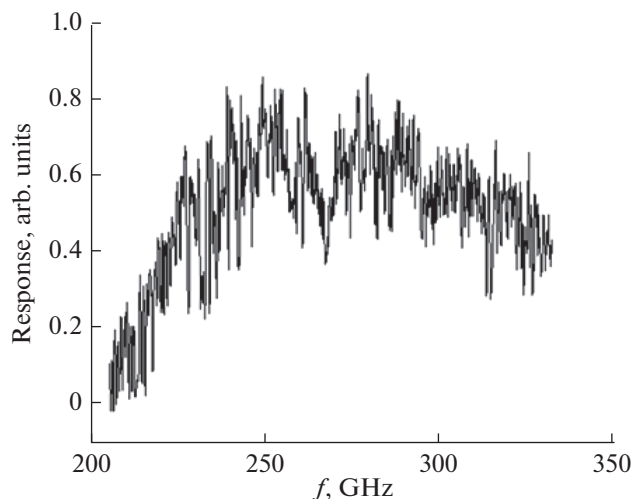


Fig. 15. Spectral response of single ring, calculated for center frequency of 240 GHz.

electric detector located outside the cryostat (see Fig. 12a). In order to more accurately measure the spectral response, additional calibration is necessary to the reference signal, which must be measured inside the cryostat. This technique was implemented in two versions: with a ruthenium-oxide-based surface-mounted resistor [13] and a sequential chain of SIN junctions. As can be seen from the experiment (Fig. 14), the array itself is a much more broadband receiver, which was shown in experiments with an immersion sapphire lens and calibration with a resistor inside the cryostat (see Fig. 14). The main calculated maximum is in the region of 350 GHz, as well as at the

subharmonics and Raman frequencies, since the elements of neighboring antennas are connected to each antenna and resonances are observed at characteristic sizes greater than half the equivalent wavelength in the dielectric at frequencies in the region of 230 and 160 GHz.

Normalization of the received signal to the response of a long sequential chain of SIN junctions and a continuous sweep of the source frequency make it possible to obtain rather smooth dependences of the received signal (Fig. 15).

CONCLUSIONS

Arrays of annular planar antennas with integrated SINIS bolometers were developed, manufactured, and experimentally investigated. To match the incoming signal with the detector, it is efficient to use an integrating cavity. It is shown that in the case of irradiation of the array from the antennas, the level of the received signal noticeably increases. To obtain a more accurate spectral response of the collecting array, additional normalization to the reference signal measured inside the cryostat is necessary.

FUNDING

This work was partially supported by the Russian Foundation for Basic Research, project no. 19-32-50002.

REFERENCES

1. P. L. Richards, *J. Appl. Phys.* **76** (1), 1 (1994).
2. W. E. Lamb, *Phys. Rev.* **70**, 308 (1946).
3. R. H. Hildebrand, *Opt. Eng.* **25**, 323 (1986).
4. N. S. Nishioka, P. L. Richards, and D. P. Woody, *Appl. Opt.* **17**, 1562 (1978).
5. C. R. Cunningham and W. K. Gear, *Instrum. in Astronomy, VII – Int. Soc. Opt. & Photon.* **1235**, 515 (1990).
6. J. Glenn, G. Chattopadhyaya, S. Edgington, et al., *Appl. Opt.* **41**, 136 (2002).
7. S. E. Church, B. Philhour, and A. E. Lnage, *Submillimetre and Far-Infrar. Space Instrum.* **388**, 77 (1996).
8. J. A. Murphy, R. Colgan, C. O'Sullivan, et al., *Infrar. Phys. Technol.* **42**, 515 (2001).
9. B. A. Munk, *Frequency Selective Surfaces: Theory and Design* (Wiley, New York, 2005).
10. S. Mahashabde, A. Sobolev, A. Bengston, et al., *IEEE Trans. Terahertz Sci. Technol.* **5**, 145 (2015).
11. V. S. Edelman, *Instrum. Exp. Tech.* **52**, 301 (2009).
12. M. A. Tarasov, V. D. Gromov, G. D. Bogomolov, et al., *Instrum and Exp. Tech.* **52**, 74 (2009).
13. S. A. Lemzyakov and V. S. Edelman, *Instrum. Exp. Tech.* **59**, 621 (2016).